Acta Crystallographica Section D
Biological Crystallography
ISSN 0907-4449

Purification, crystallization and preliminary X-ray analysis of human pirin

Q. Zeng,[a] X. Li,[a] M. Bartlam,[a] G. Wang,[a] H. Pang[a]* and Z. Rao[a,b]*

[a]Laboratory of Structural Biology, Department of Biological Science and Technology and MOE Laboratory of Protein Science, Tsinghua University, Beijing 100084, People's Republic of China, and [b]National Laboratory of Macromolecules, Institute of Biophysics, Chinese Academy of Science, Beijing 100084, People's Republic of China

Correspondence e-mail: raozh@xtal.tsinghua.edu.cn, pangh@xtal.tsinghua.edu.cn

Received 11 March 2003
Accepted 3 June 2003

Pirin is a novel highly conserved nuclear protein, but very little is known about its cellular function. Human pirin has been cloned, expressed, purified and crystallized using PEG as precipitant. The crystal belongs to the orthorhombic space group $P2_12_12_1$, with unit-cell parameters a = 42.3, b = 67.0, c = 107.3 Å, $\alpha = \beta = \gamma = 90$ Å. It contains one molecule per asymmetric unit and diffracts to 2.0 Å under cryoconditions (100 K) using an in-house Cu rotating-anode X-ray generator.

1. Introduction

Pirin is a novel protein conserved in mammals, plants, fungi and even prokaryotic organisms (Wendler *et al.*, 1997). Its N-terminal half is significantly conserved (Fig. 1). Human pirin is a 32 kDa protein consisting of 290 amino acids. Although very little is known about the cellular function of pirin, some research results indicate its potentially important role in a number of biological processes. Human pirin was initially isolated through a yeast two-hybrid screen as an interactor of nuclear factor I/CCAAT box transcription factor (NFI/CTF1), which is known to stimulate adenovirus DNA replication and RNA polymerase II-driven transcription. Pirin is exclusively localized within cell nuclei, predominantly in subnuclear dot-like structures (Wendler *et al.*, 1997).

Pirin also interacts with Bcl-3, a distinctive member of the IκB family that inhibits NF-κB. Pirin modulates p50-Bcl-3 DNA-binding activity through the formation of quarternary complexes and increases the DNA-binding activity of Bcl-3-p50 (Dechend *et al.*, 1999). The transcription factor NF-κB has been shown to participate in diverse biological processes, including embryo development, haematopoiesis and immune regulation as well as neuronal functions (Liou, 2002). It is crucial for inducing genes involved in apoptosis,

```
HUMAN           MGSSKK------VTLSVLSREQSEGVGARVRRSIGRPELKNLDPFLLFDEFKGGRP---- 50
Mouse           MASSKK------VTLSVLSREQSEGVGARVRRSIGRPELKNLDPFLLFDEFKGGKP---- 50
Tomato          MSMSSIFSRPRLVVKKVLARAQNEGDGAIVRRSIGRPELQNLDPFLMLDEFSVSQP---- 56
A.thaliana      MTYENN-SVPRIVIKKVLAKLEKEGEGAVVRNGITKIDQKLLDPFVLLVEFSFSLS---- 55
X.axonopodis    MSTTTT--TAAHVLRTIRGMPTSDGAGVKLTRVIGTQQLPELDPFLMLDEFGTDKAEDYL 58
S.oneidensis    MK----------VLGQFSAKPAMDGDGVNIRR-VADFISTQFDPFLMMDEIKSDDKQDVI 49
E.coli          MIYLRK--------ANERGHANHGWLDSWHTFSFANYYDPNFMGFSALRVINDDVIEAG- 51
                *                .       .       .       :  *  :  :  .

HUMAN           GGFPDHPHRGFETVSYLLEGGSMAHEDFCGHTGKMNPGDLQWMTAGRGILHAEMPCSEE- 109
Mouse           GGFPDHPHRGFETVSYLLEGGSMAHEDFCGHVGKMNPGDLQWMTAGRGILHAEMPCSEE- 109
Tomato          AGFPDHPHRGFETVTYMLQGA-FTHQDFAGHKGTIRTGDVQWMTAGRGIVHSEMPAGPG- 114
A.thaliana      AGFPDHPHRGFESVTYMLQGG-IIHKDPKGHKGTIQAGDVQWMTAGRGIIHSEFPEEE-- 112
X.axonopodis    AGFPSHPHRGFETVTYMLDGR-MRHKDNHGNEGLLTPGSVQWMTAGRGLIHSEMPEQESG 117
S.oneidensis    GGFPPHPHRGMETFTYIRKGG-FEHRDQMGNVKAIRTGDVQWMSTGYGVVHSEMPLADAL 108
E.coli          QGFGTHPHKDMEILTYVLEGT-VEHQDSMGNKEQVPAGEFQIMSAGTGIRHSEYNPSST- 109
                 **  ***:.:* .:*: .*  . *.*  *:   : .*..* *::* *: *:*

HUMAN           -PAHGLQLWVNLRSSEKMVEPQYQELKSEEIPKPS-KDGVTVAVISG 154
Mouse           -PAHGLQLWVNLRRSEKMVAPQYQELKSEEIPKPT-KDGVTVAVISG 154
Tomato          -TQKGLQLWINLSSKDKMIEPRYQELLHQDIPKAE-KDGVSVTILAG 159
A.thaliana      -VNNGLQLWINLPSTEKMTEPKYKELSSLDIPRAE-ENGVEVKVIAG 157
X.axonopodis    -RMRGFQLWVNLPARDKMTDPKYQEYAPDHIPVAHPASGVTVKVIAG 163
S.oneidensis    NGLHGFQIWVNMPAKDKLRPATYQDTASIPSVETTNDTGATLKALAG 155
E.coli          ERLHLYQIWIMP--EENGITPRYEQRRFDAVQGKQ-------LVLSP 147
                   .  *:*:     ::   . *::                   ::
```

Figure 1
Comparison of the N-terminal half of pirin from mammals, plants and prokaryotes. The figure was produced using *ClustalW* (Thompson *et al.*, 1994). '*' indicates positions which have a single fully conserved residue; ':' and '.' indicate positions which have a single residue with strong or weak conservation, respectively. These sequences are derived from human (*Homo sapiens*; O00625), mouse (*Mus musculus*; Q9D711), tomato (*Lycopersicon esculentum*; Q9SEE4), *Arabidopsis thaliana* (AAL83949), *Xanthomonas axonopodis* (Q8PIL5), *Shewanella oneidensis* (Q8EIE7) and *E. coli* (Q8FCQ9) pirin.

inflammation and in a wide range of diseases (Li & Verma, 2002; Chen & Shi, 2002; Sonis, 2002; Feldmann *et al.*, 2002). The stoichometry of the quaternary complexes is an important clue to elucidating the essential role played by NF-κB in cells.

Recently, it has been reported that lepirin, a tomato homologue (56% identity) of human pirin, is overexpressed during programmed cell death and that lepirin mRNA preferentially accumulates in old leaves showing symptoms of senescence. The results showed that lepirin expression is directly connected with cell death (Orzaez *et al.*, 2001). Considering the essential roles of NF-κB in apoptosis, it will probably be useful to elucidate the apoptosis pathway involved in NF-κB and pirin. Furthermore, Bergman and coworkers have revealed that pirin increases expression in RAS and c-JUN transformed cells and that inhibition of MEK1 led to reduced expression of pirin (Bergman *et al.*, 1999). These phenomena provide important clues for the cellular function of pirin.

In spite of the high conservation of pirin between mammals, plants, fungi and even prokaryotic organisms, no homologous structures have been found. Here, we report the crystallization and preliminary X-ray analysis of human pirin. Determination of its three-dimensional structure is expected to provide insight into the function of these proteins. More importantly, since the cellular function of Bcl-3 remains largely obscure, the study of its binding partner pirin will hopefully provide some valuable clues to further understanding its essential cellular functions. Pirin has also been classified as a putative NFI/CTF1 cofactor and its interaction might therefore help in obtaining new insights into the functions of NFI/CTF1.

2. Materials and methods

2.1. Cloning, overexpression and purification

The gene for pirin was amplified by PCR from a liver cDNA library. The primers for the PCR were 5′-CCGGAATTCATGGGGTCCTCCAAGAAA-3′ (forward) and 5′-TCCGCTCGAGCTAGTTCCCAATCTTTGA-3′ (reverse). The PCR product was digested with the restriction enzymes *Eco*RI and *Xho*I and ligated with the expression vector pET-28a previously digested with the same restriction enzymes. The ligation mixture was transformed into *Escherichia coli* strain BL21(DE3). A clone that overexpressed pirin was selected by SDS–PAGE and designated pET28a-pirin. The correct coding sequence of the cloned gene was verified by DNA sequencing.

A two-column procedure was developed for the purification of recombinant pirin. Briefly, 1 l of LB media containing 100 mg kanamycin was inoculated with a single colony of *E. coli* strain BL21(DE3) containing the expression construct pET28a-pirin and incubated at 310 K until an OD_{600} of 0.6 was achieved. Protein expression was induced with 0.7 m*M* isopropyl-β-D-thiogalactopyranoside at 310 K for 5 h. The cells were harvested by centrifugation and suspended in buffer *A* (30 m*M* Tris–HCl pH 8.0, 150 m*M* NaCl). The bacterial suspension was then sonicated on ice. The resulting lysate was centrifuged for 35 min at 15 000 rev min^{-1} at 277 K. The supernatant was loaded onto a 4 ml Ni–NTA column (Qiagen) equilibrated with buffer *B* (20 m*M* Tris–HCl pH 8.0, 500 m*M* NaCl) containing 10 m*M* imidazole and unbound proteins were removed by washing with 40 m*M* imidazole in Tris–HCl pH 8.0. His-tagged pirin which bound to the column was eluted from the column with buffer *B* containing 150 m*M* imidazole. The preparation was pooled and concentrated by Centricon (Millipore).

Pirin was further purified by gel-filtration chromatography on a Superdex-200 column (Pharmacia) equilibrated in 20 m*M* Tris–HCl pH 8.0 and 150 m*M* NaCl. The results of gel filtration showed pirin to exist as a stable monomer before concentration, but some dimer formation was observed as the concentration was increased (data not shown). Pirin was then concentrated to 50 mg ml^{-1} (based upon a calculated extinction coefficient of 30 560 M^{-1} cm^{-1}) using Centricon (Millipore). The protein was centrifuged through a 0.1 µm Ultrafree filter (Millipore) before use.

2.2. Crystallization

The purity of pirin was determined to be greater than 95% by SDS–gel electrophoresis. Initial screening for crystallization conditions for pirin was performed by the hanging-drop vapour-diffusion method at 277 K using Hampton Research Crystal Screen kits I and II (Jancarik & Kim, 1991) and the concentrations of pirin used in the crystallization condition search ranged from 10 to 50 mg ml^{-1}. Crystallization experiments were prepared by mixing 1.5 µl of protein solution and 1.5 µl of reservoir solution. Rod-shaped single crystals were obtained in three conditions with a protein concentration of 25 mg ml^{-1}. Condition I was 30% PEG MME 5000, 0.1 *M* MES pH 6.5 and 0.2 *M* ammonium sulfate (condition No. 26 of Crystal Screen II). Under this condition, crystals appeared after 1 d and reached their final size after about 3 d, but had poor diffraction quality. Condition II was 12% PEG 20 000, 0.1 *M* MES pH 6.5 (condition No. 22 of Crystal Screen II) and condition III was 10% PEG 8000, 0.1 *M* HEPES pH 7.5, 8% ethylene glycol (condition No. 37 of Crystal Screen II). Under the latter two conditions crystals grew slowly and reached their final size (up to 0.2 × 0.2 × 1.0 mm) after about two weeks. The best crystals were obtained by optimization of condition III and were used for data collection. However, for the selenomethionine derivative of pirin, crystals with the highest diffraction quality were obtained under condition II and the protein solution for crystallization included 10 m*M* β-mercaptoethanol.

2.3. Data collection and processing

Initial diffraction data to 2.0 Å resolution were collected under cryoconditions (100 K) using an in-house Cu rotating-anode X-ray generator. Crystals were picked up using a fibre loop and flash-frozen in a stream of cold nitrogen gas. Data from the crystal obtained from condition III were collected in-house at ∼115 K on a MAR 345 image-plate detector using Cu $K\alpha$ radiation from an in-house Rigaku rotating-anode X-ray generator operating at 48 kV and 98 mA (λ = 1.5418 Å). The freezing solution contained 20% glycerol as cryoprotectant, but was otherwise identical to the precipitant solution. The crystal-to-detector distance was 170 mm. More than 190 frames were collected and each frame was exposed for 500 s and oscillated through 1.0°. Data were processed using *DENZO* and scaled and merged using *SCALEPACK* (Otwinowski & Minor, 1997) with no σ-cutoff.

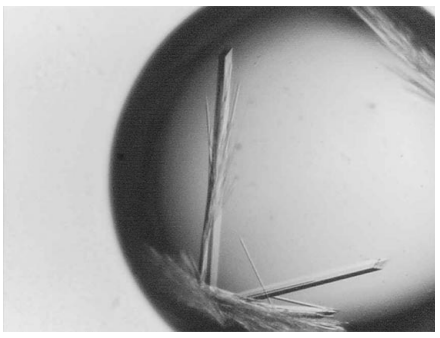

Figure 2
Photograph of the pirin crystals obtained from condition III.

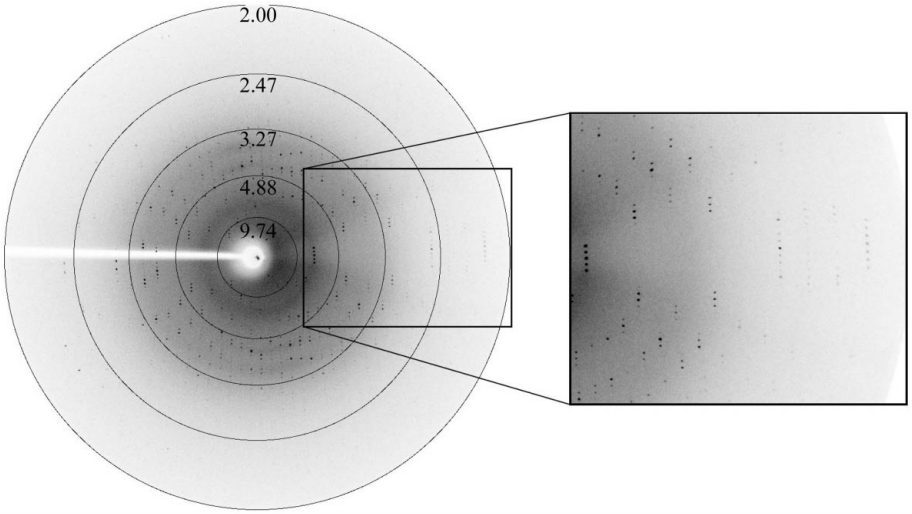

Figure 3
Sample X-ray diffraction pattern collected from condition III crystals.

3. Results

After screening a wide range of conditions, we observed that pirin crystallized under three distinct conditions. Crystals from condition I (30% PEG MME 5000, 0.1 *M* MES pH 6.5 and 0.2 *M* ammonium sulfate) were obtained after 3 d but did not diffract. Further crystals were obtained from conditions II and III after a period of two weeks. Crystals from condition II were found to diffract to 2.9 Å resolution, but the crystals were twinned and it was not possible to determine their space group. Crystals from condition III (Fig. 2) were found to diffract to 2.0 Å (Fig. 3) and a set of data was collected from this crystal. The crystals belong to the orthorhombic $P2_12_12_1$ space group, with unit-cell parameters a = 42.3, b = 63.7, c = 107.3 Å, $\alpha = \beta = \gamma = 90.0^\circ$. Scaling and merging of the crystallographic data resulted in an overall $R_{\rm merge}$ of 9.1% and an $R_{\rm merge}$ in the highest resolution shell (2.06–2.00 Å) of 58.3%. The value of the Matthews coefficient (Matthews, 1968) is 2.3 Å^3 Da^{-1} for one molecule in the asymmetric unit and the estimated solvent content is 45.1%. Complete data-collection statistics are given in Table 1.

Table 1
Data-collection statistics.

Values in parentheses correspond to the highest resolution shell.

Space group	$P2_12_12_1$
Unit-cell parameters (Å, °)	a = 42.3, b = 63.7, c = 107.3, $\alpha = \beta = \gamma$ = 90.0
Matthews coefficient (Å^3 Da^{-1})	2.3
Estimated solvent content (%)	45.1
Resolution (Å)	50–2.0 (2.06–2.0)
Total observations	65175
Unique reflections	19747 (1315)
Redundancy	3.3 (2.1)
Average $I/\sigma(I)$	3.5 (2.1)
$R_{\rm merge}$ (%)	9.1 (58.3)
Completeness	93.0 (76.5)

A selenomethionyl derivative of pirin has also been prepared and crystals have been obtained using similar conditions to those used for the native crystals. Data sets from a single selenomethionine-derivative crystal were collected at three wavelengths at 100 K on beamline 19-ID of the Advanced Photon Source (APS) at Argonne National Laboratory. Structure determination is currently under way using the MAD method.

We are grateful to Feng Gao from the Rao laboratory and to Rongguang Zhang and Andrzej Joachimiak from APS (Argonne, USA) for help with data collection. This work was supported by grants from the Ministry of Science and Technology projects '863' and '973'.

References

Bergman, A. C., Alaiya, A. A., Wendler, W., Binetruy, B., Shoshan, M., Sakaguchi, K., Bergman, T., Kronenwett, U., Auer, G., Appella, E., Jornvall, H. & Linder, S. (1999). *Cell Mol. Life Sci.* **55**, 467–471.
Chen, F. & Shi, X. (2002). *Environ. Health Perspect.* **110**, *Suppl.* 5, 807–811.
Dechend, R., Hirano, F., Lehmann, K., Heissmeyer, V., Ansieau, S., Wulczyn, F. G., Scheidereit, C. & Leutz, A. (1999). *Oncogene*, **18**, 3316–3323.
Feldmann, M., Andreakos, E., Smith, C., Bondeson, J., Yoshimura, S., Kiriakidis, S., Monaco, C., Gasparini, C., Sacre, S., Lundberg, A., Paleolog, E., Horwood, N. J., Brennan, F. M. & Foxwell, B. M. (2002). *Ann. Rheum. Dis.* **61**, *Suppl.* 2, ii13–ii18.
Jancarik, J. & Kim, S.-H. (1991). *J. Appl. Cryst.* **24**, 409–411.
Li, Q. & Verma, I. M. (2002). *Nature Rev. Immunol.* **2**, 725–734.
Liou, H. C. (2002). *J. Biochem. Mol. Biol.* **35**, 537–546.
Matthews, B. W. (1968). *J. Mol. Biol.* **33**, 491–497.
Orzaez, D., de Jong, A. J. & Woltering, E. J. (2001). *Plant Mol. Biol.* **46**, 459–468.
Otwinowski, Z. & Minor, W. (1997). *Methods Enzymol.* **276**, 307–326.
Sonis, S. T. (2002). *Crit. Rev. Oral Biol. Med.* **13**, 380–389.
Thompson, J. D., Higgins, D. G. & Gibson, T. J. (1994). *Nucleic Acids Res.* **22**, 4673–4680.
Wendler, W. M., Kremmer, E., Forster, R. & Winnacker, E. L. (1997). *J. Biol. Chem.* **272**, 8482–8489.